Cherrypicking resolvents: A general strategy for convergent coupled-cluster damped response calculations of core-level spectra

Kaushik D. Nanda[a,*] and Anna I. Krylov[a,†]

[a] Department of Chemistry, University of Southern California, Los Angeles, California 90089-0482

* kaushikdnanda@gmail.com (K.D.N.), † krylov@usc.edu (A.I.K.)

Damped linear response calculations within the equation-of-motion coupled-cluster singles and doubles (EOM-CCSD) framework usually diverge in the X-ray regime. This divergent behavior stems from the valence ionization continuum in which the X-ray response states are embedded. Here, we introduce a general strategy for removing the continuum from the response manifold while preserving the important spectral properties of the model Hamiltonian. The strategy is based on decoupling the core and valence Fock spaces using the core–valence separation (CVS) scheme, followed by separate (approximate) treatment of the core and valence resolvents. We illustrate this approach with the calculations of resonant inelastic X-ray scattering spectra of benzene and *para*-nitroaniline using EOM-CCSD wave functions and several choices of resolvents, which differ in their treatment of the valence manifold. The method shows robust convergence and extends the previously introduced CVS-EOM-CCSD RIXS scheme to systems for which valence contributions to the total cross section are important, such as the push–pull chromophores with charge-transfer states.

Equation-of-motion coupled-cluster (EOM-CC) theory[1–6] provides a robust single-reference framework for computing multiple electronic states. EOM-CC affords a balanced description of states of different characters and a systematic improvement of the results by the incremental improvement in treating electron correlation. The EOM-CC hierarchy of approximations is based on the standard hierarchy of the CC models for the ground state, such as CC singles (CCS), the approximate CC singles and doubles[7] (CC2), CC with singles and doubles[2,8–10] (CCSD), CC with singles, doubles, and triples (CC3[11] and CCSDT[12]), and so on. The EOM-CC formalism naturally extends to state and transition properties. Together, these features make EOM-CC an ideal framework for spectroscopy modeling. EOM-CC can be used to compute solvatochromic shifts[13], transition dipole moments[2], spin–orbit[14–17] and non-adiabatic[18–20] couplings, photoionization cross sections[21,22], and higher-order properties[23] such as two-photon absorption cross sections[24–27] and static and dynamic polarizabilities[28–31].

The EOM-CC framework is being vigorously extended to the X-ray regime, for modeling X-ray absorption (XAS), photoionization, and emission spectra[32–37], as well as multi-photon phenomena, such as resonant inelastic X-ray scattering[38–42] (RIXS) (Fig. 1). The successful extensions of EOM-CC to the X-ray domain exploit the core–valence separation (CVS) scheme[43], which effectively addresses the key challenge in the theoretical treatment of core-level states—their resonance nature due to the coupling with the valence ionization continuum. Being embedded in the continuum, the core-level states, strictly speaking, cannot be treated by methods developed for isolated bound states with L^2-integrable wave functions[44]. Practically, the coupling with the continuum leads to erratic and often divergent behavior of the solvers, the lack of the systematic convergence of the results with the basis-set increase, and often unphysical solutions[44,45]. The CVS scheme allows one to separate the continuum of valence states from the core-level states by a deliberate pruning of the Fock space, i.e., by removing the configurations that can couple core-excited (or core-ionized) states with the valence continuum. CVS can be described as a diabatization approach, separating the bound part of the resonance from the continuum, as done in the Feshbach–Fano treatment of the resonances. In other words, the couplings between the core- and valence excited (or ionized) determinants are omitted from the model EOM-CC Hamiltonian. The eigenstates of such a reduced EOM-CC Hamiltonian are either purely valence or purely core excited (or ionized). The purely core-excited (or ionized) states become formally bound because of the uncoupling with the valence determinants forming the valence continuum. The core CVS-EOM-CC Hamiltonian, obtained by projecting out the purely valence block of

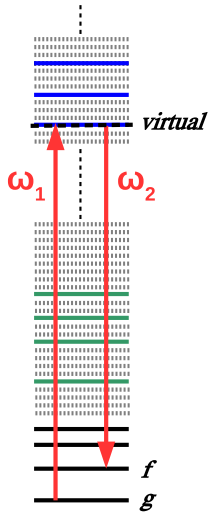

FIG. 1. In the coherent RIXS process, an incoming x-ray photon of energy ω_1 (resonant with a core-excited state) is absorbed and an outgoing x-ray photon of energy ω_2 is emitted. The difference between the two photon energies equals the excitation energy of the final valence state f relative to the initial state g. The process is often described in terms of a transition via a virtual state (black dashed line), which represents collective contributions from all electronic states of the system, including the valence bound states (solid black), valence resonances (green), core-excited states (blue), and valence continuum states (ultrafine dashed in grey).

this reduced EOM–CC Hamiltonian, provides a robust means for smoothly convergent calculations of core-excited (or core-ionized) states.

Initially used to describe core-level states, the CVS scheme was recently extended into the response domain[39–41], to enable calculations of RIXS transition moments within the damped linear response theory[46–49] and the EOM-CCSD method for excitation energies (EOM-EE-CCSD). In this CVS-EOM-EE-CCSD extension, the response equations are solved in the truncated Fock space spanning the singly and doubly excited determinants in which at least one orbital belongs to the core[39,40]. Thus, all valence excited states are excluded, which can be justified by the resonant nature of RIXS process. This strategy, which works well in many situations, is expected to break down when the off-resonance contributions to the RIXS cross section from the valence states become important. At least one class of systems where this happens is the push–pull chromophores featuring low-lying charge-transfer states[41].

Here, we address this limitation of the previous formulation of RIXS theory within the CVS-EOM-CCSD framework and present a general strategy for obtaining converged RIXS response states that also include off-resonance valence contribution to the RIXS signal. This strategy also applies to modeling other multiphoton X-ray processes, such as X-ray two-photon absorption.

The derivation of the equations for RIXS transition moments between the initial (g) and final (f) states starts from the Kramers–Heisenberg–Dirac formula[50,51], which translates to the following sum-over-states (SOS) expressions[38–42] within the EOM-EE-CCSD damped response theory:

$$\begin{aligned} &M_{xy}^{f\leftarrow g}(\omega_{1x}+i\varepsilon,-\omega_{2y}-i\varepsilon) \\ &\quad=-\sum_{n\geq 0}\left(\frac{\langle\Phi_0\mathcal{L}^f|\bar{\mu}_y|\mathcal{R}^n\Phi_0\rangle\langle\Phi_0\mathcal{L}^n|\bar{\mu}_x|\mathcal{R}^g\Phi_0\rangle}{\mathcal{E}_n-\mathcal{E}_g-\omega_{1x}-i\varepsilon}\right. \\ &\quad\left.+\frac{\langle\Phi_0\mathcal{L}^f|\bar{\mu}_x|\mathcal{R}^n\Phi_0\rangle\langle\Phi_0\mathcal{L}^n|\bar{\mu}_y|\mathcal{R}^g\Phi_0\rangle}{\mathcal{E}_n-\mathcal{E}_g+\omega_{2y}+i\varepsilon}\right) \end{aligned} \tag{1}$$

and

$$\begin{aligned} &M_{xy}^{g\leftarrow f}(-\omega_{1x}+i\varepsilon,\omega_{2y}-i\varepsilon) \\ &\quad=-\sum_{n\geq 0}\left(\frac{\langle\Phi_0\mathcal{L}^g|\bar{\mu}_x|\mathcal{R}^n\Phi_0\rangle\langle\Phi_0\mathcal{L}^n|\bar{\mu}_y|\mathcal{R}^f\Phi_0\rangle}{\mathcal{E}_n-\mathcal{E}_g-\omega_{1x}+i\varepsilon}\right. \\ &\quad\left.+\frac{\langle\Phi_0\mathcal{L}^g|\bar{\mu}_y|\mathcal{R}^n\Phi_0\rangle\langle\Phi_0\mathcal{L}^n|\bar{\mu}_x|\mathcal{R}^f\Phi_0\rangle}{\mathcal{E}_n-\mathcal{E}_g+\omega_{2y}-i\varepsilon}\right). \end{aligned} \tag{2}$$

Here, $\mathcal{T}$ is an excitation operator containing the CCSD amplitudes and $\bar{\mu}=e^{-\mathcal{T}}\mu e^{\mathcal{T}}$ is the similarity-transformed dipole moment. $\mathcal{L}^n$ and $\mathcal{R}^n$ are the EOM-CCSD left and right excitation operators, respectively[52], for state n with energy $\mathcal{E}_n$. Their amplitudes and respective eigenenergies are found by diagonalizing the EOM-CCSD similarity-transformed Hamiltonian $\bar{\mathcal{H}}=e^{-\mathcal{T}}\mathcal{H}e^{\mathcal{T}}$ in the respective sector of the Fock space (i.e., singly and doubly excited determinants in EOM-EE-CCSD)

$$\bar{\mathcal{H}}\mathcal{R}^n=E_n\mathcal{R}^n \quad\text{and}\quad \mathcal{L}^n\bar{\mathcal{H}}=\mathcal{L}^nE_n. \tag{3}$$

$i\varepsilon$ is the phenomenological damping (or inverse lifetime) term of the damped response theory. ω_{1x} and ω_{2y} are the x-polarized absorbed and y-polarized emitted frequencies satisfying the RIXS resonance condition

$$\omega_1-\omega_2=\mathcal{E}_f-\mathcal{E}_g. \tag{4}$$

We drop the Cartesian indices of the photon frequencies for brevity.

The Fock space of EOM-EE-CCSD comprises Slater determinants Φ_ρ, where $\rho\in\{\text{reference},\ CV,\ OV,\ COVV,\ CCVV,\ OOVV\}$ and C, O, and V denote the core occupied, valence occupied, and unoccupied orbitals, respectively. Upon inserting the identity operator ($\mathbf{1}=\sum_\rho|\Phi_\rho\rangle\langle\Phi_\rho|$) in Eqs. (1) and (2), we obtain

$$\begin{aligned} &M_{xy}^{f\leftarrow g}(\omega_1+i\varepsilon,-\omega_2-i\varepsilon)=-\sum_\rho \\ &\left(\langle\tilde{\mathcal{D}}_y^f|\Phi_\rho\rangle\langle\Phi_\rho|\mathcal{X}_{x,\omega_1+i\varepsilon}^g\rangle+\langle\tilde{\mathcal{D}}_x^f|\Phi_\rho\rangle\langle\Phi_\rho|\mathcal{X}_{y,-\omega_2-i\varepsilon}^g\rangle\right) \end{aligned} \tag{5}$$

and

$$\begin{aligned} &M_{xy}^{g\leftarrow f}(-\omega_1+i\varepsilon,\omega_2-i\varepsilon)=-\sum_\rho \\ &\left(\langle\tilde{\mathcal{D}}_x^g|\Phi_\rho\rangle\langle\Phi_\rho|\mathcal{X}_{y,\omega_1-i\varepsilon}^f\rangle+\langle\tilde{\mathcal{D}}_y^g|\Phi_\rho\rangle\langle\Phi_\rho|\mathcal{X}_{x,-\omega_2+i\varepsilon}^f\rangle\right), \end{aligned} \tag{6}$$

where the amplitudes of the intermediate $\tilde{\mathcal{D}}_y^k$ and the first-order response wave function $\mathcal{X}_{x,\omega_1+i\varepsilon}^k$ for state k are given by[24,39]

$$\langle\tilde{\mathcal{D}}_y^k|\Phi_\rho\rangle=\langle\Phi_0\mathcal{L}^k|\bar{\mu}_y|\Phi_\rho\rangle \tag{7}$$

and

$$\langle\Phi_\rho|\mathcal{X}_{x,\omega+i\varepsilon}^k\rangle=\sum_n\langle\Phi_\rho|\mathcal{R}^n\Phi_0\rangle\frac{\langle\Phi_0\mathcal{L}^n|\bar{\mu}_x|\mathcal{R}^k\Phi_0\rangle}{\mathcal{E}_n-\mathcal{E}_g-(\omega+i\varepsilon)}. \tag{8}$$

The response wave function in Eq. (8) is complex and given by a linear combination of all EOM-CCSD states. The amplitudes of this response wave function, expressed in the basis of Slater determinants, are solutions of the following response equation:

$$\sum_\rho\langle\Phi_\nu|\bar{\mathcal{H}}-\mathcal{E}_g-(\omega+i\varepsilon)|\Phi_\rho\rangle\langle\Phi_\rho|X_{x,\omega+i\varepsilon}^k\rangle=\langle\Phi_\nu|\mathcal{D}_x^k\rangle, \tag{9}$$

where the amplitudes of intermediate $\mathcal{D}_x^k$ are given by

$$\langle\Phi_\nu|\mathcal{D}_x^k\rangle=\langle\Phi_\nu|\bar{\mu}_x|\mathcal{R}^k\Phi_0\rangle. \tag{10}$$

Eq. (9) is a direct result of using the identity operator $\mathbf{1}=\sum_n|\mathcal{R}^n\Phi_0\rangle\langle\Phi_0\mathcal{L}^n|$ and the following resolvent:

$$\begin{aligned} &\sum_{n\geq 0}\frac{\langle\Phi_\rho|\mathcal{R}^n\Phi_0\rangle\langle\Phi_0\mathcal{L}^n|\Phi_\nu\rangle}{\mathcal{E}_n-\mathcal{E}_g-\omega-i\varepsilon} \\ &\quad=\langle\Phi_\rho|\left(\bar{\mathcal{H}}-\mathcal{E}_g-\omega-i\varepsilon\right)^{-1}|\Phi_\nu\rangle. \end{aligned} \tag{11}$$

In practice, response equations such as Eq. (9) are solved iteratively, using standard procedures such as the Direct Inversion in the Iterative Subspace[53] (DIIS) relying on diagonal

preconditioners. In the X-ray regime, such response equations often diverge, due to three reasons[39,40]. First, owing to its resonant nature, the RIXS response wave function in Eq. (8) is often dominated by contributions from high-lying core-excited states that are nearly resonant with the absorbed photon's energy. These high-lying states are embedded inside the valence ionization continuum and are Feshbach resonances that are metastable with respect to electron ejection. Mathematically, these core-excited states (and consequently, the response state) are strongly coupled to the continuum via the doubly excited determinants, which leads to the oscillatory behavior of these response amplitudes with large magnitudes in the course of the iterative procedure. Second, similarly to the core-excited states, the valence resonances are also strongly coupled to the continuum via the doubly excited determinants, resulting in erratic behavior of the corresponding purely valence doubly excited response amplitudes. Third, whereas the coupling terms between valence doubly excited determinants (off-diagonal terms of valence doubles–doubles block of $\bar{\mathcal{H}}$) in EOM-CCSD and higher correlated methods are important to create a high density of states of the valence continuum, for high-energy photons, this leads to the diagonal preconditioner for the valence doubly excited amplitudes to be no longer a good approximation to the valence doubles–doubles block of $\bar{\mathcal{H}} - \mathcal{E}_g - (\omega + i\varepsilon)$.

We note that lower-level theories such as CIS[54] and TDDFT[55–58] do not have valence double excitations in the excitation manifold, so that the issue with the convergence of response equations in the X-ray regime does not arise, simply because there is no valence continuum. Similarly, this issue does not arise for theories such as ADC(2)[59,60] and CC2 in which the doubly excited configurations are not coupled[39,40] (valence doubles–doubles block is diagonal), so the high-lying valence states are sufficiently discrete and the diagonal preconditioner for the doubles–doubles block is exact.

The first practical solution for these convergence problems, which plague higher-level many-body approaches, was introduced in Refs. 39 and 40 and implemented within the CVS-EOM-EE-CCSD framework. The target EOM states obtained by diagonalizing the similarity-transformed CVS-EOM-EE-CCSD Hamiltonian ($\bar{H}$) are either purely valence excited or purely core excited. Eq. (8) in terms of these CVS-EOM-EE-CCSD states is given according to the following direct sum:

$$\langle \Phi_\rho | \mathcal{X}^k_{x,\omega+i\varepsilon} \rangle \approx \langle \Phi_\xi | X^{k,val}_{x,\omega+i\varepsilon} \rangle \oplus \langle \Phi_\lambda | X^{k,core}_{x,\omega+i\varepsilon} \rangle; \quad (12)$$

$$\langle \Phi_\xi | X^{k,val}_{x,\omega+i\varepsilon} \rangle = \sum_n^{val} \langle \Phi_\xi | R^n \Phi_0 \rangle \frac{\langle \Phi_0 L^n | \bar{\mu}_x | \mathcal{R}^k \Phi_0 \rangle}{E_n - E_g - (\omega + i\varepsilon)}; \quad (13)$$

$$\langle \Phi_\lambda | X^{k,core}_{x,\omega+i\varepsilon} \rangle = \sum_n^{core} \langle \Phi_\lambda | R^n \Phi_0 \rangle \frac{\langle \Phi_0 L^n | \bar{\mu}_x | \mathcal{R}^k \Phi_0 \rangle}{E_n - E_g - (\omega + i\varepsilon)}, \quad (14)$$

where ξ spans the reference and the valence excitation manifold (OV and OOVV configurations) and λ spans the core excitation manifold (CV, COVV, and CCVV configurations). The L and R in the sum over core-excited states are left and right CVS-EOM-CCSD operators for the core-excited state n with energy E_n that diagonalize the core CVS-EOM-EE-CCSD similarity-transformed Hamiltonian ($\bar{H}^{core} = e^{-T} H^{core} e^{T}$). T is the CCSD operator. Similarly, the sum over valence states (including the reference CCSD state with energy E_g) involves the EOM operators that diagonalize the valence Hamiltonian ($\bar{H}^{val}$) with the core states projected out. In terms of resolvents, the amplitudes of the response state in Eq. (12) are given by

$$\langle \Phi_\xi | X^{k,val}_{x,\omega+i\varepsilon} \rangle = \sum_\zeta \langle \Phi_\xi | \left(\bar{H}^{val} - E_g - \omega - i\varepsilon \right)^{-1} | \Phi_\zeta \rangle \langle \Phi_\zeta | \mathcal{D}^k_x \rangle; \quad (15)$$

$$\langle \Phi_\lambda | X^{k,core}_{x,\omega+i\varepsilon} \rangle = \sum_\kappa \langle \Phi_\lambda | \left(\bar{H}^{core} - E_g - \omega - i\varepsilon \right)^{-1} | \Phi_\kappa \rangle \langle \Phi_\kappa | \mathcal{D}^k_x \rangle, \quad (16)$$

where ζ spans the reference and the valence excitation manifold and κ spans the core excitation manifold. The core resolvent is given according to

$$\begin{aligned} &\langle \Phi_\lambda | \left(\bar{H}^{core} - E_g - \omega - i\varepsilon \right)^{-1} | \Phi_\kappa \rangle \\ &= \sum_{n>0}^{core} \frac{\langle \Phi_\lambda | R^n \Phi_0 \rangle \langle \Phi_0 L^n | \Phi_\kappa \rangle}{E_n - E_g - \omega - i\varepsilon} \\ &= \langle \Phi_\chi | \left(\bar{H} - E_g - \omega - i\varepsilon \right)^{-1} | \Phi_\tau \rangle \\ &\quad \ominus \frac{\langle \Phi_0 | \Phi_0 \rangle \langle \Phi_0 \left(1 + \Lambda_\kappa \right) | \Phi_\tau \rangle}{E_0 - E_g - \omega - i\varepsilon}, \end{aligned} \quad (17)$$

where χ and τ span the reference and the core excitation space[39].

Second, in the approach presented in Ref. 39 (we call it the CVS-0 approach here), the sum in Eq. (12) is truncated to span over core-excited states only. This is justified as the contributions of nearly resonant core-excited states to the RIXS moments are dominant for most RIXS transitions, given the resonant nature of RIXS. The numerical convergence of response state, now approximated as

$$\langle \Phi_\rho | \mathcal{X}^k_{x,\omega+i\varepsilon} \rangle \approx \langle \Phi_\lambda | X^{k,core}_{x,\omega+i\varepsilon} \rangle, \quad (18)$$

is smooth, given that the continuum has been projected out by the CVS mechanism. The numeric benchmarks have shown that for the systems for which the response equations could be converged with the standard EOM-EE-CCSD resolvent, this scheme results in the RIXS spectra that were very close to the full, untruncated calculation[39].

Whereas this approach for computing RIXS spectra within the CVS-EOM-CCSD framework is justified for systems with RIXS transitions characterized by contributions from nearly resonant core-excited states, in Ref. 41, we have shown counterexamples of push–pull chromophores such as para-nitroaniline and 4-amino-4'-nitrostilbene for which off-resonance valence states contribute to the RIXS moments. The CVS-EOM-CCSD calculation with the CVS-0 resolvent neglects these contributions and is insufficient for modeling the RIXS spectra of such systems. Here, we provide a general strategy for including the contributions from valence states to the damped linear response in the X-ray regime, while preventing the direct coupling of the response states with the

continuum and thus, preserving robust convergence of the response equations.

The response equation for $X^{k,val}$ is given according to

$$\sum_{\xi}\langle\Phi_\zeta|\bar{H}^{val}-E_g-(\omega+i\varepsilon)\,|\Phi_\xi\rangle\langle\Phi_\xi|X^{k,val}_{x,\omega+i\varepsilon}\rangle = \langle\Phi_\zeta|\mathcal{D}^k_x\rangle, \tag{19}$$

As explained above, the convergence of the above response equation is compromised due to the coupling between the valence resonances with the continuum and the use to diagonal preconditioner for the *OOVV*–*OOVV* block of $\bar{H}^{val}$. The continuum can be projected out by omitting the singles–doubles and doubles–singles blocks from the CVS-EOM-EE-CCSD $\bar{H}^{val}$. By further ignoring the doubles–doubles block of $\bar{H}^{val}$, the corresponding preconditioner is no longer needed in the iterative procedure. Indices ξ and ζ now span just the reference and the *OV* excited configurations, reducing the resolvent such that $X^{k,val}$ is given as a linear combination of states obtained by the action of EOM operators, $R = r_0 + R_1$ and $L = L_1$, on the CCSD reference. The response equation for this CVS plus valence uncoupled singles approach (we call it the CVS-uS approach), which effectively ignores the doubles amplitudes of $X^{k,val}$, is given by

$$\sum_{\xi}^{0,OV}\langle\Phi_\zeta|\bar{H}^{val}-E_g-(\omega+i\varepsilon)\,|\Phi_\xi\rangle\langle\Phi_\xi|X^{k,val}_{x,\omega+i\varepsilon}\rangle = \langle\Phi_\zeta|\mathcal{D}^k_x\rangle \tag{20}$$

Note that omitting just the *OOVV* component from $\mathcal{D}^k_x$ in Eq. (19) does not project out the valence resonances from the continuum nor does it exclude the use of the problematic doubles–doubles preconditioner. Therefore, any strategy to include the valence contribution to the RIXS moments must involve the response solution and the model Hamiltonian (or the resolvent).

Another way to include the contributions from valence states approximated by single excitations is to express the response state in Eq. (13) in terms of the valence CVS-EOM-EE-CCS intermediate states with the CCS reference. This amounts to replacing the valence CVS-EOM-EE-CCSD resolvent in Eq. (13) by the valence CVS-EOM-EE-CCS resolvent as follows:

$$\langle\Phi_\rho|X^{k,val}_{x,\omega+i\varepsilon}\rangle \approx \langle\Phi_\lambda|\mathtt{X}^{k,val}_{x,\omega+i\varepsilon}\rangle; \tag{21}$$

$$\sum_{\xi}^{0,OV}\langle\Phi_\zeta|\bar{\mathtt{H}}^{val}-\mathtt{E}_0-(E_g-E_0)-(\omega+i\varepsilon)\,|\Phi_\xi\rangle \langle\Phi_\xi|\mathtt{X}^{k,val}_{x,\omega+i\varepsilon}\rangle = \langle\Phi_\zeta|\mathcal{D}^k_x\rangle \tag{22}$$

where the $\bar{\mathtt{H}}^{val}$ is the CVS-EOM-EE-CCS similarity-transformed Hamiltonian, $\mathtt{E}_0$ is the energy of CCS reference, and $\mathtt{X}^{k,val}$ is the corresponding approximated $X^{k,val}$. Because doubly excited configurations are not present in this low-level CVS-EOM-EE-CCS Hamiltonian, its spectrum does not contain continuum states, which, as discussed above, does not result in problematic convergence of RIXS response states. We call this the CVS-CCS approach.

Yet another alternative entails replacing the valence CVS-EOM-EE-CCSD resolvent by the valence resolvent from the CVS-EOM-EE-CC2 model; we call this the CVS-CC2 approach. The CVS-EOM-EE-CC2 Hamiltonian has a diagonal doubles–doubles block; therefore, it spans continuum states that do not couple with each other via the doubly excited determinants, yielding a rather discretized continuum. Similarly, the valence resonances (and indeed, core resonances) do not couple to the continuum via the doubly excited determinants. In addition, the preconditioner used for *OOVV* amplitudes in the iterative procedures for solving the response equations is exact. Indeed, as noted in Refs. 39 and 40, the CC2 linear response RIXS solutions do not diverge. We exploit this feature of CC2 to compute the valence response amplitudes in Eq. (22). These new approaches—CVS-uS, CVS-CCS, and CVS-CC2—are implemented in a development version of the Q-Chem electronic structure package[61,62].

In principle, the strategy of simply replacing the valence CVS-EOM-EE-CCSD resolvent by a resolvent of lower-level method that avoids the erratic convergence of RIXS response solutions can also be extended to CIS, ADC(2), and DFT resolvents, for example. Note that both the core and valence resolvents can be cherrypicked separately after enforcing the CVS scheme. This "cherrypicking-of-resolvents" strategy exploits the better convergence of the X-ray response equations within the framework of the lower-level method, while using the better energies and wave functions of the initial and final states computed at the higher EOM-CCSD level of theory.

We begin by comparing the RIXS spectra computed using different resolvents for a well behaved case, benzene; the RIXS spectrum of benzene with the CVS-0 approach is discussed in detail in Ref. 39. Fig. 2 shows the spectra computed for resonant excitation of two brightest XAS peaks, peak A corresponding to a core$\rightarrow\pi^*$ transition and peak B corresponding to a core$\rightarrow Ry$ transition. As one can see, the CVS-0 approach captures all main features in the emission following peak A excitation and inclusion of the valence block does not have noticeable effect. For peak B, small differences appear in minor peaks when compared to the CVS-0 results; the valence contributions become somewhat important due to the Rydberg character of the particle orbital and the smaller oscillator strength for the peak-B core excitation. The CVS-CCS and CVS-uS approaches give similar peak intensities and differ slightly from the CVS-CC2 results. Another example (water) is given in the SI.

Fig. 3 compares the RIXS emission spectra for *para*-nitroaniline using the CVS-EOM-EE-CCSD framework in Ref. 39 for the different resolvents. Here, the incident photon frequency is resonant with the lowest $XA_1 \rightarrow B_2$ core excitation at 285.88 eV, which corresponds to the dominant X-ray absorption peak (see SI).

With the CVS-0 approach, we observe a few small inelastic features in the RIXS spectrum. These features correspond to the $XA_1 \rightarrow 1B_2$, $XA_1 \rightarrow 2A_2$, $XA_1 \rightarrow 3B_1$, and $XA_1 \rightarrow 4A_2$

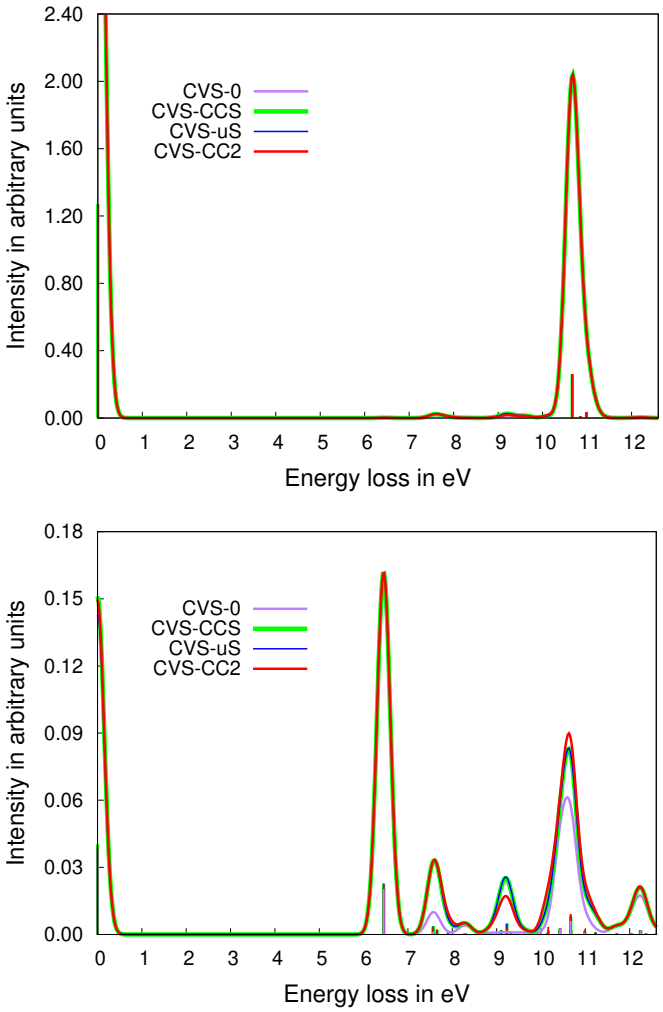

FIG. 2. RIXS emission spectra for benzene computed using different resolvents within the CVS-EOM-EE-CCSD framework with (top) pumping peak A (285.97 eV) and (bottom) pumping peak B (287.80 eV) for scattering angle $\theta = 0^\circ$ and 6-311(2+,+)G**(uC) basis[39,63]. The spectra are convoluted using normalized Gaussians (FWHM = 0.25 eV).

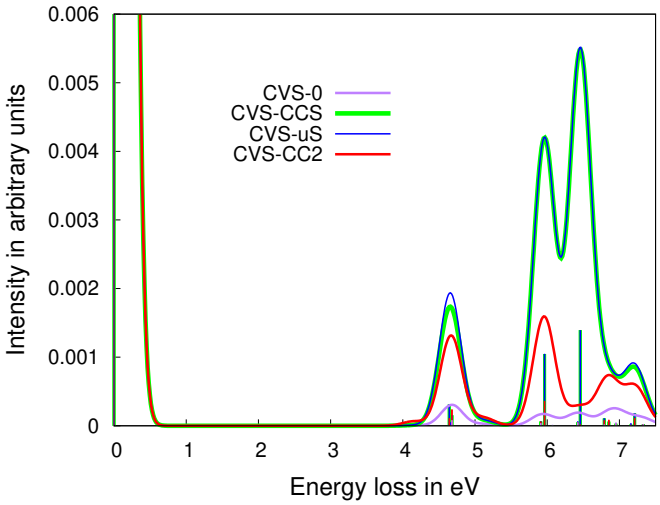

FIG. 3. RIXS emission spectra for *para*-nitroaniline for the incident photon resonant with the lowest core excitation ($XA_1 \rightarrow B_2$), scattering angle $\theta = 0^\circ$, 6-311(2+,+)G**(uC) basis, and computed within the CVS-EOM-EE-CCSD framework using different resolvents. The spectra are convoluted using normalized Gaussian functions (FWHM = 0.25 eV).

transitions at 4.68 eV, 5.91 eV, 6.42 eV, and 6.95 eV energy loss, respectively; the $XA_1 \rightarrow 1B_2$ being the most dominant (see the SI for raw data).

For the CVS-uS and CVS-CCS approaches, the computed RIXS spectra are similar. However, these two approaches give different dominant features compared to the CVS-0 approach. Although the dominant $XA_1 \rightarrow 1B_2$ transition in the CVS-0 approach is still important in the RIXS spectra with these approaches, it is no longer the dominant feature. Rather, the two dominant features arise from the $XA_1 \rightarrow 3B_1$ and $XA_1 \rightarrow 2B_1$ transitions at 6.46 eV and 5.96 eV, respectively. Other transitions, such as the $XA_1 \rightarrow 1B_1$ at 4.64 eV, $XA_1 \rightarrow 4B_2$ at 6.79 eV, and $XA_1 \rightarrow 5B_2$ at 7.21 eV, also give non-negligible contribution to the RIXS spectra.

Next, we compare the spectra obtained with the CVS-0 and CVS-CC2 approaches. Whereas the former spectrum is dominated by the $XA_1 \rightarrow 1B_2$ transition, the latter also shows other transitions such as $XA_1 \rightarrow 1B_1$, $XA_1 \rightarrow 2B_1$, $XA_1 \rightarrow 4B_2$, $XA_1 \rightarrow 3A_2$ (at 6.85 eV), and $XA_1 \rightarrow 5B_2$. We note that the relative cross sections of these RIXS transitions are also different with the $XA_1 \rightarrow 2B_1$ having the largest cross section.

The comparison of the RIXS spectra of *para*-nitroaniline with CVS-0 and with valence resolvents highlights the significance of off-resonance contributions from the valence states to the X-ray signal. The RIXS spectra computed with the CVS-CC2 approach differs significantly from the CVS-CCS and CVS-SDS approaches. This is not surprising as it is well known from previous benchmarks[64] that valence two-photon absorption cross sections with CCS and CC2 response theory show stark differences. The choice of the valence resolvent within this framework, in addition to comparison with experiments, is subject to the ability of the model valence Hamiltonian to provide a balanced description of the full spectrum of states for the specific system.

In conclusion, we have presented a novel general strategy for obtaining converged response states in the X-ray regime, specifically in the context of RIXS, within the EOM-EE-CCSD damped response theory framework. Whereas the iterative procedure for computing EOM-EE-CCSD response states typically diverges in the X-ray regime due to the coupling of response states with the continuum, our strategy mitigates this issue by exploiting the CVS scheme that decouples the valence excitation block from the core-excitation block of the EOM-EE-CCSD Hamiltonian, which facilitates computing their contributions to the RIXS response separately. Refs. 39 and 40 have previously presented a EOM-EE-CCSD damped response theory approach that employs the damped CVS-EOM-EE-CCSD resolvent for computing the contribution from the core-excited states; here, we introduced a more general strategy to include the contributions from valence ex-

cited states. This strategy involves the replacement of the valence CVS-EOM-EE-CCSD resolvent in the expression of the response state with a resolvent from a lower-level theory (such as CVS-EOM-CCS or CVS-EOM-CC2) for which the response equations do not diverge or by restricting the valence CVS-EOM-EE-CCSD resolvent to the singly excited determinant space. We demonstrated the significance of including this off-resonance valence contribution to the RIXS cross section by comparing the RIXS emission spectra of *para*-nitroaniline computed with and without the different valence resolvents.

SUPPLEMENTARY MATERIAL

This document contains the raw data for RIXS spectra of water, benzene, and *para*-nitroaniline, XAS data for *para*-nitroaniline, and the geometries and basis sets used.

ACKNOWLEDGMENTS

This work was supported by the U.S. National Science Foundation (No. CHE-1856342).

CONFLICTS OF INTEREST

A.I.K. is the President and a part-owner of Q-Chem, Inc.

DATA AVAILABILITY STATEMENT

The data that supports the findings of this study are available within the article [and its supplementary material].

[1]Emrich, K. An extension of the coupled-cluster formalism to excited states (I) *Nucl. Phys.* **1981**, *A351*, 379–396.

[2]Stanton, J. F.; Bartlett, R. J. The equation of motion coupled-cluster method. A systematic biorthogonal approach to molecular excitation energies, transition probabilities, and excited state properties *J. Chem. Phys.* **1993**, *98*, 7029–7039.

[3]Krylov, A. I. Equation-of-motion coupled-cluster methods for open-shell and electronically excited species: The hitchhiker's guide to Fock space *Annu. Rev. Phys. Chem.* **2008**, *59*, 433–462.

[4]Bartlett, R. J. The coupled-cluster revolution *Mol. Phys.* **2010**, *108*, 2905–2920.

[5]Sneskov, K.; Christiansen, O. Excited state coupled cluster methods *WIREs: Comput. Mol. Sci.* **2012**, *2*, 566–584.

[6]Bartlett, R. J. Coupled-cluster theory and its equation-of-motion extensions *WIREs: Comput. Mol. Sci.* **2012**, *2*, 126–138.

[7]Christiansen, O.; Koch, H.; Jørgensen, P. The 2nd-order approximate coupled-cluster singles and doubles model CC2 *Chem. Phys. Lett.* **1995**, *243*, 409–418.

[8]Sekino, H.; Bartlett, R. J. A linear response, coupled-cluster theory for excitation energy *Int. J. Quant. Chem.* **1984**, *26*, 255–265.

[9]Koch, H.; Jørgensen, P. Coupled cluster response functions *J. Chem. Phys.* **1990**, *93*, 3333–3344.

[10]Koch, H.; Jensen, H.J.Aa.; Jørgensen, P.; Helgaker, T. Excitation energies from the coupled clusters singles and doubles linear response functions (CCSDLR). Applications to Be, CH^+, CO, and H_2O *J. Chem. Phys.* **1990**, *93*, 3345–3350.

[11]Christiansen, O.; Koch, H.; Jorgensen, P. Response functions in the CC3 iterative triple excitation model *J. Chem. Phys.* **1995**, *103*, 7429–7441.

[12]Noga, J.; Bartlett, R.J. The full CCSDT model for molecular electronic structure *J. Chem. Phys.* **1987**, *86*, 7041–7050.

[13]Slipchenko, L. V. Solvation of the excited states of chromophores in polarizable environment: Orbital relaxation versus polarization *J. Phys. Chem. A* **2010**, *114*, 8824–8830.

[14]Christiansen, O.; Gauss, J.; Schimmelpfennig, B. Spin-orbit coupling constants from coupled-cluster response theory *Phys. Chem. Chem. Phys.* **2000**, *2*, 965–971.

[15]Klein, K.; Gauss, J. Perturbative calculation of spin-orbit splittings using the equation-of-motion ionization-potential coupled-cluster ansatz *J. Chem. Phys.* **2008**, *129*, 194106.

[16]Epifanovsky, E.; Klein, K.; Stopkowicz, S.; Gauss, J.; Krylov, A. I. Spin-orbit couplings within the equation-of-motion coupled-cluster framework: Theory, implementation, and benchmark calculations *J. Chem. Phys.* **2015**, *143*, 064102.

[17]Pokhilko, P.; Epifanovsky, E.; Krylov, A. I. General framework for calculating spin–orbit couplings using spinless one-particle density matrices: theory and application to the equation-of-motion coupled-cluster wave functions *J. Chem. Phys.* **2019**, *151*, 034106.

[18]Tajti, A.; Szalay, P.G. Analytic evaluation of the nonadiabatic coupling vector between excited states using equation-of-motion coupled-cluster theory *J. Chem. Phys.* **2009**, *131*, 124104.

[19]Ichino, T.; Gauss, J.; Stanton, J. F. Quasidiabatic states described by coupled-cluster theory *J. Chem. Phys.* **2009**, *130*, 174105.

[20]Faraji, S.; Matsika, S.; Krylov, A. I. Calculations of non-adiabatic couplings within equation-of-motion coupled-cluster framework: Theory, implementation, and validation against multi-reference methods *J. Chem. Phys.* **2018**, *148*, 044103.

[21]Gozem, S.; Gunina, A. O.; Ichino, T.; Osborn, D. L.; Stanton, J. F.; Krylov, A. I. Photoelectron wave function in photoionization: Plane wave or Coulomb wave? *J. Phys. Chem. Lett.* **2015**, *6*, 4532–4540.

[22]Gozem, S.; Seidel, R.; Hergenhahn, U.; Lugovoy, E.; Abel, B.; Winter, B.; Krylov, A. I.; Bradfort, S. E. Probing the electronic structure of bulk water at the molecular length scale with angle-resolved photoelectron spectroscopy *J. Phys. Chem. Lett.* **2020;** in press; https://dx.doi.org/10.1021/acs.jpclett.0c00968.

[23]Helgaker, T.; Coriani, S.; Jørgensen, P.; Kristensen, K.; Olsen, J.; Ruud, K. Recent advances in wave function-based methods of molecular-property calculations *Chem. Rev.* **2012**, *112*, 543–631.

[24]Nanda, K. D.; Krylov, A. I. Two-photon absorption cross sections within equation-of-motion coupled-cluster formalism using resolution-of-the-identity and Cholesky decomposition representations: Theory, implementation, and benchmarks *J. Chem. Phys.* **2015**, *142*, 064118.

[25]Nanda, K. D.; Krylov, A. I. Effect of the diradical character on static polarizabilities and two-photon absorption cross-sections: A closer look with spin-flip equation-of-motion coupled-cluster singles and doubles method *J. Chem. Phys.* **2017**, *146*, 224103.

[26]Nanda, K. D.; Krylov, A. I. Visualizing the contributions of virtual states to two-photon absorption cross-sections by natural transition orbitals of response transition density matrices *J. Phys. Chem. Lett.* **2017**, *8*, 3256–3265.

[27]Nanda, K. D.; Krylov, A. I. The effect of polarizable environment on two-photon absorption cross sections characterized by the equation-of-motion coupled-cluster singles and doubles method combined with the effective fragment potential approach *J. Chem. Phys.* **2018**, *149*, 164109.

[28]Rozyczko, P. B.; Perera, S. A.; Nooijen, M.; Bartlett, R. J. Correlated calculations of molecular dynamic polarizabilities *J. Chem. Phys.* **1997**, *107*, 6736–6747.

[29]Hättig, C.; Christiansen, O.; Coriani, S.; Jørgensen, P. Static and frequency-dependent polarizabilities of excited singlet states using coupled cluster response theory *J. Chem. Phys.* **1998**, *109*, 9237.

[30]Nanda, K. D.; Krylov, A. I. Static polarizabilities for excited states within the spin-conserving and spin-flipping equation-of-motion coupled-cluster singles and doubles formalism: Theory, implementation, and benchmarks *J. Chem. Phys.* **2016**, *145*, 204116.

[31]Nanda, K. D.; Krylov, A. I.; Gauss, J. COMMUNICATION: The pole structure of the dynamical polarizability tensor in equation-of-motion coupled-cluster theory *J. Chem. Phys.* **2018**, *149*, 141101.

[32]Coriani, S.; Christiansen, O.; Fransson, T.; Norman, P. Coupled-cluster response theory for near-edge x-ray-absorption fine structure of atoms and molecules *Phys. Rev. A* **2012**, *85*, 022507.

[33]Zuev, D.; Vecharynski, E.; Yang, C.; Orms, N.; Krylov, A. I. New algorithms for iterative matrix-free eigensolvers in quantum chemistry *J. Comput. Chem.* **2015**, *36*, 273–284.

[34]Coriani, S.; Koch, H. Communication: X-ray absorption spectra and core-ionization potentials within a core-valence separated coupled cluster framework *J. Chem. Phys.* **2015**, *143*, 181103.

[35]Coriani, S.; Koch, H. Erratum: "Communication: X-ray absorption spectra and core-ionization potentials within a core-valence separated coupled cluster framework" [J. Chem. Phys. 143, 181103 (2015)] *J. Chem. Phys.* **2016**, *145*, 149901.

[36]Vidal, M. L.; Feng, X.; Epifanovski, E.; Krylov, A. I.; Coriani, S. A new and efficient equation-of-motion coupled-cluster framework for core-excited and core-ionized states *J. Chem. Theory Comput.* **2019**, *15*, 3117–3133.

[37]Loh, Z.-H.; Doumy, G.; Arnold, C.; Kjellsson, L.; Southworth, S. H.; Al Haddad, A.; Kumagai, Y.; Tu, M.-F.; Ho, P. J.; March, A. M.; Schaller, R. D.; Bin Mohd Yusof, M. S.; Debnath, T.; Simon, M.; Welsch, R.; Inhester, L.; Khalili, K.; Nanda, K. D.; Krylov, A. I.; Moeller, S.; Coslovich, G.; Koralek, J.; Minitti, M. P.; Schlotter, W. F.; Rubensson, J.-E.; Santra, R.; Young, L. Observation of the fastest chemical processes in the radiolysis of water *Science* **2020**, *367*, 179–182.

[38]Faber, R.; Coriani, S. Resonant inelastic X-ray scattering and nonesonant X-ray emission spectra from coupled-cluster (damped) response theory *J. Chem. Theory Comput.* **2019**, *15*, 520–528.

[39]Nanda, K. D.; Vidal, M. L.; Faber, R.; Coriani, S.; Krylov, A. I. How to stay out of trouble in RIXS calculations within the equation-of-motion coupled-cluster damped response theory framework? Safe hitchhiking in the excitation manifold by means of core-valence separation *Phys. Chem. Chem. Phys.* **2020**, *22*, 2629–2641.

[40]Faber, R.; Coriani, S. Core–valence-separated coupled-cluster-singles-and-doubles complex-polarization-propagator approach to X-ray spectroscopies *Phys. Chem. Chem. Phys.* **2020**, *22*, 2642–2647.

[41]Nanda, K. D.; Krylov, A. I. A simple molecular orbital picture of RIXS distilled from many-body damped response theory *J. Chem. Phys.* **2020**, *152*, 244118.

[42]Kjellsson, L.; Nanda, K. D.; Rubensson, J.-E.; Doumy, G.; Southworth, S. H.; Ho, P. J.; March, A. M.; Al Haddad, A.; Kumagai, Y.; Tu, M.-F.; Debnath, T.; Bin Mohd Yusof, M. S.; Arnold, C.; Schlotter, W. F.; Moeller, S.; Coslovich, G.; Koralek, J. D.; Minitti, M. P.; Vidal, M. L.; Simon, M.; Santra, R.; Loh, Z.-H.; Coriani, S.; Krylov, A. I.; Young, L. Resonant inelastic x-ray scattering reveals hidden local transitions of the aqueous OH radical *Phys. Rev. Lett.* **2020**, *124*, 236001.

[43]Cederbaum, L. S.; Domcke, W.; Schirmer, J. Many-body theory of core holes *Phys. Rev. A* **1980**, *22*, 206.

[44]Jagau, T.-C.; Bravaya, K. B.; Krylov, A. I. Extending quantum chemistry of bound states to electronic resonances *Annu. Rev. Phys. Chem.* **2017**, *68*, 525–553.

[45]Sadybekov, A.; Krylov, A. I. Coupled-cluster based approach for core-ionized and core-excited states in condensed phase: Theory and application to different protonated forms of aqueous glycine *J. Chem. Phys.* **2017**, *147*, 014107.

[46]Buckingham, A.D.; Fischer, P. Phenomenological damping in optical response tensors *Phys. Rev. A* **2000**, *61*, 035801–035804.

[47]Kristensen, K.; Kauczor, J.; Thorvaldsen, A. J.; Jørgensen, P.; Kjaergaard, T.; Rizzo, A. Damped response theory description of two-photon absorption *J. Chem. Phys.* **2011**, *134*, 214104–214120.

[48]Norman, P. A perspective on non resonant and resonant electronic response theory for time-dependent molecular properties *Phys. Chem. Chem. Phys.* **2011**, *12*, 20519–20535.

[49]Kauczor, J.; Norman, P.; Christiansen, O.; Coriani, S. Communication: A reduced-space algorithm for the solution of the complex linear response equations used in coupled cluster damped response theory *J. Chem. Phys.* **2013**, *139*, 211102.

[50]Kramer, H.A.; Heisenberg, W. Über die streuung von strahlung durch atome *Z. Phys.* **1925**, *31*, 681–708.

[51]Dirac, P.A.M. The quantum theory of the emission and absorption of radiation *Proc. R. Soc. London* **1927**, *114*, 243–265.

[52]Levchenko, S. V.; Krylov, A. I. Equation-of-motion spin-flip coupled-cluster model with single and double substitutions: Theory and application to cyclobutadiene *J. Chem. Phys.* **2004**, *120*, 175–185.

[53]Pulay, P. *Chem. Phys. Lett.* **1980**, *73*, 393.

[54]Foresman, J.B.; Head-Gordon, M.; Pople, J.A.; Frisch, M.J. Toward a systematic molecular orbital theory for excited states *J. Phys. Chem.* **1992**, *96*, 135–149.

[55]Runge, E.; Gross, E.K.U. Density-functional theory for time-dependent systems *Phys. Rev. Lett.* **1984**, *52*, 997–1000.

[56]Hanson-Heine, M. W. D.; George, M. W.; Besley, N. A. Kohn-Sham density functional theory calculations of non-resonant and resonant x-ray emission spectroscopy *J. Chem. Phys.* **2017**, *146*, 094106.

[57]Jensen, L.; Autschbach, J.; Schatz, G. C. Finite lifetime effects on the polarizability within time-dependent density-functional theory *J. Chem. Phys.* **2005**, *122*, 224115.

[58]Kauczor, J.; Norman, P. Efficient calculations of molecular linear response properties for spectral regions *J. Chem. Theory Comput.* **2014**, *10*, 2449–2455.

[59]Rehn, D.R.; Dreuw, A.; Norman, P. Resonant inelastic X-ray scattering amplitudes and cross sections in the algebraic diagrammatic construction/intermediate state representation (ADC/ISR) approach *J. Chem. Theory Comput.* **2017**, *13*, 5552–5559.

[60]Norman, P.; Dreuw, A. Simulating X-ray spectroscopies and calculating core-excited states of molecules *Chem. Rev.* **2018**, *118*, 7208–7248.

[61]Krylov, A. I.; Gill, P. M. W. Q-Chem: An engine for innovation *WIREs: Comput. Mol. Sci.* **2013**, *3*, 317–326.

[62]Shao, Y.; Gan, Z.; Epifanovsky, E.; Gilbert, A.T.B.; Wormit, M.; Kussmann, J.; Lange, A.W.; Behn, A.; Deng, J.; Feng, X., et al. Advances in molecular quantum chemistry contained in the Q-Chem 4 program package *Mol. Phys.* **2015**, *113*, 184–215.

[63]Sarangi, R.; Vidal, M. L.; Coriani, S.; Krylov, A. I. On the basis set selection for calculations of core-level states: Different strategies to balance cost and accuracy *Mol. Phys.* **2020;** in press; DOI https://doi.org/10.1080/00268976.2020.1769872.

[64]Paterson, M.J.; Christiansen, O.; Pawlowski, F.; Jørgensen, P.; Hättig, C.; Helgaker, T.; Salek, P. Benchmarking two-photon absorption with CC3 quadratic response theory, and comparison with density-functional response theory *J. Chem. Phys.* **2006**, *124*, 054332.